تعميم طريقة المعامل لتتبع الفيضانات خلال خزانات السدود

الدكتور غازي المشهداني

كلية الهندسة– جامعة الموصل

ملخص البحث :

تحوي الدراسة على محاولة رياضية لتعميم طريقة المعامل لتتبع الفيضانات خلال خزانات السدود وذلك بافتراض ان العلاقة بين الخزن المؤقت والتصريف الخارج من الخزان علاقة لاخطية. وبناء على ذلك تقترح الدراسة طريقة تجريبية رياضية للتعامل مع المسألة.

GENERALISATION OF COEFFICIENT METHOD FOR ROUTING A FLOOD THROUGH A RESERVOIR

By

Dr. G. AL MASHIDANI

ABSTRACT

The coefficient method has been generalised by assuming a nonlinear relationship between storage and outflow. An empirical procedure for the solution of general equation has been developed. The method of solution was found to yield reasonable results.

https://doi.org/10.30684/etj.1983.1.2
2412-0758/University of Technology-Iraq, Baghdad, Iraq
This is an open access article under the CC BY 4.0 license http://creativecommons.org/licenses/by/4.0

INTRODUCTION

Coefficient method[1,2] of reservoir routing is well known. It is easy to apply since there is no need of initial curves to be prepared as is required in other graphical procedures . The method is based on the general continuity equation as used in other techniques, but, further, assumes that storage is directly proportional to the outflow . An equation can thus be derived which gives the outflow at a given time step as a function of average inflow, outflow at previous time step and the constant of propoprtionality, K, of storage outflow relationship. The assumption that storage is directly proportional to the outflow is usually not true in a real field problem, hence it is customary to use, K, as a variable (Chow 1964) the values of which can be determined for various segments of storage versus discharge curve, although in so doing the ease with which coefficient method can be applied is lost. The present paper is an attempt to modify the coefficient method by assuming a non-linear relationship between storage and outflow .

Development of the method

Assuming a non – linear relationship between storage, S, and outflow, Q, one can write

$$S = KQ^n \qquad \ldots\ldots (1)$$

where ,n, and ,K, are constants which can be determined by usual regression technique given in equations(2) and (3) if some outflow values are known for the corresponding storage values.

$$n = \frac{\Sigma (\ln S - \overline{\ln S})(\ln Q - \overline{\ln Q})}{\Sigma (\ln Q - \ln Q)^2} \qquad \ldots\ldots (2)$$

$$\text{and } K = \overline{\ln S} - n \overline{\ln Q} \qquad \ldots\ldots (3)$$

The continuity equation for reservoir routing is written as follows :

$$\frac{1}{2} (I_i + I_{i+1}) t - \frac{1}{2} (Q_i + Q_{i+1}) t = S_{i+1} - S_i \qquad \ldots\ldots (4)$$

where suffix i and i + 1 represent the state of inflow I, outflow Q and storage S before and after a chosen time step t. Combining eq. (1) and (4) it can be shown that

$$\frac{2K}{t} Q^n_{i+1} + Q_{i+1} = (I_{i+1} + I_i) + \left(\frac{2K}{t} Q^n_i - Q_i \right) \qquad \ldots\ldots (5)$$

The only unknown in eq. (5) is, Q_{i+1}, which can be solved by trial and error.

The solution of eq. (5) by trial and error although straight forward is time consuming, such that an empirical solution procedure wnich gives reasonable results has been developed.

General procedure for solution

Eq. (5) can be rewritten as :

$$Q_{i+1} = \left[\frac{(I_{i+1} + I_i) + \left(\frac{2K}{t} Q^n_i - Q_i \right)}{\frac{2K}{t} + Q^{1-n}_{i+1}} \right]^{\frac{1}{n}} \qquad \ldots\ldots (6)$$

In eq. (6) if a small time step is chosen the value of. $\frac{2K}{t}$. is much larger than. Q_{i+1}. hence even if the value of . Q_{i+1}^{1-n} . in the denominator is replaced by an approximate value, it does not affect the result significantly. Thus, the value of . Q_{i+1}^{1-n} . in denominator of eq. (6) is replaced by. $(\bar{Q}_{i+1})^{1-n}$ the value of which can again be calculated from eq. (6) by replacing the unknown term' Q_{i+1}^{1-n}' in the denominator by its value at previous time interval as is shown in eq. (7) and (8). Thus an approximate solution of eq. (5) can be written as :

$$Q_{i+1} = \left[\frac{(I_{i+1} + I_i) + \left(\frac{2K}{t} Q_i^n - Q_i \right)}{\frac{2K}{t} + (\bar{Q}_{i+1})^{1-n}} \right]^{\frac{1}{n}} \quad \ldots\ldots\ldots\ldots (7)$$

where.

$$(\bar{Q}_{i+1}) = \left[\frac{(I_{i+1} + I_i) + \left(\frac{2K}{t} Q_i^n - Q_i \right)}{\frac{2K}{t} + Q_i^{1-n}} \right]^{\frac{1}{n}} \quad \ldots\ldots\ldots\ldots (8)$$

Two numerical examples have been solved by following the above procedure. the solutions have been compared with results obtained from other procedures.

Details of numerical example

Ist Example :- The value of inflow flood hydrograph is shown in table 1 for Ist example. The storage outflow relationship for this example can be written as :

$$S = 302200\, Q^{0.82055}.$$

Thus the value of $k = 302200$ and $n = 0.82055$ a time step of 12 hours ($= 12 \times 3600$ sec) has been chosen for analysis.

The values of $\bar{Q}_{i+1}$ and Q_{i+1} along with corresponding values of Q_{i+1} calculated by step by step method (Varshney. 1977) are given in table 1. It can be seen that the two values are very close to each other. The values of Q_{i+1} . calculated in Col. (4) has also been found to satisfy eq. (5).

IInd Example : - The second example is based on the data taken from Bekhme Reservoir (Urban. 1967) on Greater Zab river in North of Iraq. The storage outflow relationship for this case is given in table 2 and can be represented by

$$S = 419529.86\, Q^{0.8476593} + 1.95 \times 10^{11}.$$

Thus the value of K and n. are 419529.86 and 0.8476593. The value of time step chosen here again is 12 hours. The outflow hydrograph for this example has also been calculated by conventional* coefficient method using variable value of K (details are shown in table 2). The values of outflow. Q_{i+1}. as calculated from eq. (7) here again has been found to satisfy eq. (5).

---

* The conventional coefficient method means herein the coefficient method in general use as $Q_{i+1} = Q_i + \left(\frac{2t}{2K + t} \right) \left(\frac{I_{i+1} + I_i}{2} - Q_i \right)$

Table 1. Results of Example 1 : —

Time hours	Inflow $1 m^3$/ sec	Approx . values Q_{i+1}	Outflow Q_{i+1} m^3/sec	Values of Q_{i+1} by step by step method
	0	0	0	0
	127.5	14.77	14.77	14.2
	350.4	95.70	80.11	71.0
	736.0	253.18	243.96	241.0
	1700.0	725.36	695.80	695.0
	1050.0	1020.03	1003.67	977.0
	732.0	951.16	951 74	905.0
	510.0	795.71	801.78	780.0
	325.0	625.94	632.36	651.0
	198.5	469.22	474.81	481.0
	99.3	337.73	342.12	340.0
	42.5	233.81	237.03	227.0
	0	155.73	157.96	142.0
		102.06	103.49	99.3
		69.08	69.92	
		47.99	48.50	

Table 2. Values of , K , and Coefficient , C , for Conventional Coefficient method .

Outflow m^3/ sec	Storage m^3	K	Coefficient $C = \frac{1}{\left(K / \Delta t + \frac{1}{2} \right)}$
	1.95×10^9	140000	0.2673
	2.09×10^9	130000	0.28496
	2.22×10^9	115000	0.31625
	2.45×10^9	95000	0.3705
	2.64×10^9	75000	0.4473
	2.79×10^9	70,000	0.4176
	2.93×10^9		

Table 3. Results of example 2.

Time hours	Inf ow 1 m^3/sec	Approx . values Q_{i+1} eq. (8)	Outflow Q_{i+1} eq. (7)	Outflow by conventional coefficient method method
	1000	1000	1000	1000
	1250	1038	1037	1033
	2000	1218	1214	1202
	3500	1705	1691	1643
	7000	2900	2861	2671
	10200	4951	4877	4546
	8000	6488	6435	6233
	5600	6576	6572	6487
	4500	5986	6003	5844

156	3950	5328	5346	5244
168	3600	4759	4774	4700
180	3300	4286	4299	4237
192	3100	3899	3909	3853

Discussion and Conclusions :

It can be seen that the method requires no graphs to be plotted . as errors due to graphical plotting . choice of scale etc . are eliminated . Besides . the method appears to be sufficiently general and can be easily programmed. For the two examples worked out in the present case the results obtained are comparable to those obtained by other methods . The values calculated by Eq . (7) satisfied eq. (5) reasonably well . even the approximate values worked out by eq . (8) give results which are close to that of eq . (7) .

References

1. Al-Taie . M. Y.. 1979. "Reservoir and Channel Routing". M. Sc. Thesis. College of Engineering . University of Mosul . Iraq .
2. Chow . V. T.. 1964 . "Statistical and Probability Analysis of Hydrologic data" . page 25 - 40 Handbook of Applied Hydrology . Chow . ed . : McGraw Hill . New York .
3. Urban . J.. 1967 . "Flood Routing in Reservoirs " Report. Faculty of Engineering . University of Mosul . Iraq .
4. Varshney. R. S.. 1977. "Engineering Hydrlogy". New Chand & Brothers . 2nd Edition . Roorkee .

Nomenclature :

S = Storage
Q = Outflow
K = Constant of proportionality in storage outflow relationship
n = Exponent of outflow in storage out flow erlationship
I = Inflow
i and i+1 are suffixes indicating state of event before and after a time step t
t = time step
In S = average value of natural logarithm of storage
In Q = average value of natural logarithm of outflow values
$\bar{Q}$ = Approximate value of outflow Q .

STRESS DISTRIBUTION IN A WEDGE INDENTOR

BY
Dr. M.I. Ghobrial

توزيع الاجهادات في أداة ثلم اسفينية الشكل

بقلم
الدكتور مجدي ابراهيم غبريال
الجامعة التكنولوجية –بغداد

خلاصة المقالة :

لقد بينت التحليلات المبنية على أساس نظرية اللدونة أنه خلال عمليه الثلم بواسطة اداة اسفينية الشكل ، يتعرض سطحي مماسي الاسفين الى اجهاد عمودي منتظم ، واجهاد آلي منتظم. ويقدم هذا البحث دراسة نظرية حول توزيع الاجهادات في الاسفين عند تعرضه لمثل اجهادات التماس هذه. ويظهر الحل النهائي على شكل معادلات تكاملية وقد استخدمت في ذلك طريقة «ترانتر» التي تعتمد على محولات « ملن » التكاملية.

STRESS DISTRIBUTION IN A WEDGE INDENTOR

by
Dr.M.I. Ghobrial

Summary :

Plasticity analysis for orthogonal wedge indentation of plastic rigid material suggests that the faces of the wedge will be subjected to uniformly distributed pressure and tangential stress over the contact length. In the present work the stress distribution at the tip of an infinitely deep wedge is obtained when the wedge is subjected to such a stress distribution. The problem simulates the industrial scoring process for the manufacturing of easy open can tops. The solution is obtained in integral form using a method proposed by Tranter, which is based on the application of Mellin Integral Transform.

Notation:

P_0	normal pressure	
K	shear yield strength	
E	modulus of elasticity	
τ	shear stress	
T_0	frictional shear stress	
μ	coefficient of friction	
σ_θ , σ_r	normal stresses	polar co-ordinates
$T_{r\theta}$	shear stress	polar co-ordinates
γ	radial co-ordinate	polar co-ordinates
σ_x , σ_r	normal stresses	cartesian co-ordinates
τ_{xy}	shear stress	cartesian co-ordinates
α , ψ , θ	angles	

1 –INTRODUCTIN :

The industrial Scoring* process presents a number of unsolved problems related to the wear or fracture of the tool tip. For these problems to be solved it will be necessary to obtain detailed information on the stress distribution in the indenting tool under surface loadingsimilar to those encountered in the scoring process. In industry it has been usual to effect scoring of the can ends by the use of a Crank press in which a scoring tool is fixed rigidly to a ram which is caused to penetrate can ends. The process, is therefore,approximately a plane strain indentation problem. The most conventional tool profile used for scoring aluminium can ends was the trapezoidal wedge [1] having an included angle of 50° and a flat width of 0.002 in to 0.007 in. Tools with such profile were found, in practice, to have a relatively short life when used for scoring ferrous metals such as tin-plate and to be subject to fracture at the corners. It has therefore, been replaced in the last few yearsby sharp-edged wedges[2] having a total included angle of 90 . This, however, proved also to be not very satisfactory [1]

The primary object of the present work is to obtain basic information on the nature of stress distribution in the region where fatigue-crack nucleation or surface wear occurs. For this reason the general equations for stress distributions throughout a sharp-edged wedge are evaluated for boundary conditions approximating to the loads on sharp-edged wedge indenter. The distributions of stress are represented in terms of trigonometric integrals with the aid of a method proposed by Tranter [3] which is based on the application of the Mellin Integral Transforms. Full description of this method is contained in references[3] and[4] and, therefore, details are not repeated here.

2- STRESS BOUNDARY CONDITIONS IN SHARP–EDGED WEDGE INDENTATION :

The process to be considered is one in which a flat strip or sheet of plastic-rigid material is indented by means of a tool. The tool spans the width of the strip and the width/thickness ratio of the strip is large enough for edge effects to be neglected The flow is confined to planes perpendicular to the tool and the deformation is assumed to take place under plane - strain conditions . As the tool advances into the material , two stages of the operation can be distinguished :

(a) Surface indentation.
(b) Deep Penetration.

Surface indentation is an elastic-plastic mode of deformation and at this stage the bulk of the indented material is elastic. However, after a certain critical depth the plastically stressed region reaches the foundation. This stage is defined as Deep-penetration. Hill, Lee and Tupper[5] initiated aslip-line field solution forthe surface indentation of a semi-infinite block of plastic rigid material by frictionless acute angled wedge . This field is shown in figure[1] and is characterised by two isosceles triangles and a fan. The configuration is geometrically similar at every stage and the field merely changes in size as the deformation proceeds. This filed suggests that the normal pressure acting on the surfaces of the tool,will be uniformly distributed over the contact length and is given by the equation. [5]

$$p = 2k (1 + \psi)$$

* "Scoring" is the industrial name for the indentation process of metal can ends .

where 'K' is the shear yield stress of the indented material. The angle' ψ ' of the slip-line field is related to the wedge semi-angle' α' by the relation[5]:

$$\frac{h}{d} = \{ \cos\alpha - \sin(\alpha - \psi) \}^{-1}$$

Thus, the magnitude of the uniformly distributed pressure acting on the wedge faces depends on the tool geometry and the yield stress of the material and is not affected by the variation of the depth of indentation.

Grunzweig, Longman and Petch[6] have given the solution for plane strain surface indentation of a plastic rigid material by a rough (Coulomb friction) wedge. The slip-line field of this solution is shown in figure (2) and the relationship between $\alpha, \psi, \lambda, \mu$ and c which are given by Grunzweig[6] can be found from the requirements of continuing geometrical similarity and incompressibility. The normal compressive stress 'p' and the shearing stress 'τ' acting on the wedge are given by the relations:

$$p = k(1 + 2\psi + \sin 2\lambda)$$

$$\tau = k \cos 2\lambda$$

Consequently the coefficient of friction is given by :

$$\mu = \cos 2\lambda / (1 + 2\psi + \sin 2\lambda)$$

A limit occurs in this field when $(\alpha - \lambda) > \pi/4$, since the yield criterion should not be violated in the rigid region near the point B, Figure 2. If $\alpha > \pi/4$ then the indenter will be covered with a 90° wedge shaped dead metal cap. The slip-line field for this case has been presented and calculated by Johnson, Mahtab and Haddow[7] It should be noted, however, that for wide angled wedges elastic effects become important. This has been discussed by Mulhearn [3] and March [9], whereas Hirst and Howse [10] idealised the process of blunt-wedge indentation by the elastic expansion of cylind rical cavity in an infinite medium.

It is therefore, possible to conclude that the theoretical plasticity analysis suggessts that for frictionless acute angled wedge indentation the normal pressure acting on the wedge face is uniformly distributed and fo rough acute-angled wedge indentation (Coulomb friction) both normal pressure and tangential stresses are uniformly distributed. However, two conditions are to be satisfied;

a- The included angle of the wedge must be acute.
b- The ratio E/Y for the indented material must be high (i.e. plastic – rigid materi

In the following work, Tranter's method is used to find the stress distributions in an infinite wedge when subjected to such boundary conditions. The method could be applied directly to the problem of finding the stresses in the wedge for uniform distribution of normal pressure and shear stress. However, the algebra involved in reducing the Mellin inversion integrals to trigonometric form is considerably simplified by first solving for uniformly distributed normal pressure and then for uniformly tangential boundary stresses.
The solution for the stress distributions in wedge indentation is then obtained by superposition of the two solutions. The procedure is represented schematically in Figure (3).

3- THE SOLUTION

A- Application of Uniform Normal Pressure to The Faces of an Infinite Wedge :

Using polar coordinates the distribution of stress in an infinite wedge of semiangle 'α' when its faces are each subjected to a uniform pressure p_0, acting on both faces of the wedge for a distance A measured from the vertex, was found to be represented by the following equations :

$$\frac{\pi r}{2AP_0}(\sigma_\theta - \sigma_r) = \frac{\sin\alpha\cos\theta}{2\alpha + \sin 2\alpha} - \int_0^\infty P(u)\sin\left[u\ln\left(\frac{A}{r}\right)\right]du \qquad \ldots(1)$$

$$\frac{\pi r}{2AP_0}(\sigma_\theta + \sigma_r) = \frac{-\pi\sin(\alpha)\cos(\theta)}{2\alpha + \sin(2\alpha)} + \int_0^\infty [P(u) - uQ(u)]\sin\left[u\ln\left(\frac{A}{r}\right)\right] -$$

$$-[Q(u) + uP(u)]\cos\left[u\ln\left(\frac{A}{r}\right)\right]\frac{du}{1+u^2} \qquad \ldots(2)$$

$$\frac{\pi r}{AP_0}\tau_{r\theta} = \int_0^\infty R(u)\cos\left[u\ln\left(\frac{A}{r}\right)\right]du \qquad \ldots\ldots(3)$$

where the functions P (u), Q (u) and R (u) are given by

$$(u\sin 2\alpha + \sinh 2\alpha\, u)\,P(u) = \sin(\alpha-\theta)\cosh(\alpha+\theta)u + \sin(\alpha+\theta)\cosh(\alpha-\theta)u$$

$$(u\sin 2\alpha + \sinh 2\alpha u)\,Q(u) = \cos(\alpha-\theta)\sinh(\alpha+\theta)u + \cos(\alpha+\theta)\sinh(\alpha-\theta)u$$

$$(u\sin 2\alpha + \sinh 2\alpha u)\,R(u) = \sin(\alpha-\theta)\sinh(\alpha+\theta)u - \sin(\alpha+\theta)\sinh(\alpha-\theta)u$$

The values of the stress components were evaluated numerically for a wedge angle $2\alpha = 60°$ and $2\alpha = 90°$ Simpson formula was used for high ratios of A/r. Computations were stopped very close to the wedge tip where the ratio A/r tends to infinity giving indeterminate stress at the apex of the wedge. All the integrals were computed over equal intervals of θ from $\theta = \alpha$ to $\theta = -\alpha$ and the stress distribution in the form of $(\sigma_\theta - \sigma_r)$, $(\sigma_\theta + \sigma_r)$ and $\tau_{r\theta}$ were evaluated. This enabled the construction of contours of equal maximum shear stress (Isochromat ics) and the results are shown in Figurs (4) and (5). The contours of equal directions of principal stresses (Isoclin ics) for a (90° wedge are presented in Figure (6) and it enabled the construction of the Isostatic pattern presented in Figure (7) Several theoretical results are of interest. An isotropic region is seen to extend across the wedge to join the two points at the two faces of the wedge where $r = A$. Above this isotropic region the maximum shear stress increases sharply and reaches its peak value on the axis of symmetry at a distance equal to $A(\sin\alpha + \cos\alpha)$ from the apex.

Below the isotropic region, the order of isochromatic increases continuously toward the apex. It is clear from from inspection of Figure (7) that within this region both radial and tangential stresses are compressive.

The radial stress distribution on the faces of a wedge were evaluated numerically from either of equations (1) or (2) for wedge angles of $2\alpha = 60^\circ$ and $2\alpha = 90^\circ$ and the results are shown in Figures (8) and (9). It can be seen that a finite stress discontinuity of magnitude P exists at $r = A$. In practice, such stress discontinuity would not be expected. However, it is reasonable to assume that the radial stress drops rapidly at a small distance within $r = A$

The variation of maximum shear stress across different sections perpendicular to this axis of symmetry are also indicated in Figures (8) and (9). The variation of radial and tangential stress along the axis of symmetry are also represented in these figures, and because of symmetry the shear stress $\tau_{r\theta}$ is equal to zero. Except for a small region at the apex the radial stresses σ_r are compressive all along the axis of symmetry. Within the small region at the wedge apex the tangential stresses tend to be infinite. This physically unrealistic result represents a breakdown in this present type of solution within a small region enclosing the apex. However, in practice this region may be regarded as a zone of incipient plastic deformation.

II- Application of Uniform Shear Stress to the Faces of an Infinite Wedge :

With the use of Trantters method, the stress distribution in an infinite wedge loaded on both Faces on the segment $r < A$ by uniform shear stress was found to be represented by the following equations :

$$\frac{\pi r}{2AT_0}(\sigma_\theta - \sigma_r) = \frac{\pi \cos\alpha \cos\theta}{2\alpha + \sin 2\alpha} - \int_0^\infty [\, z(u) - u\, Y(u)\,] \left[\sin\left(u \ln \frac{A}{r} \right) - u \cos\left(u \ln \frac{A}{r} \right) \right] \frac{du}{1+u^2}$$

$$\frac{\pi r}{2AT_0}(\sigma_\theta - \sigma_r) = \frac{-\pi \cos\alpha \cos\theta}{2\alpha + \sin 2\alpha} + \int_0^\infty \left[[\, z(u) + Y(u)\,] \sin\left(u \ln \frac{A}{r} \right) + [\, -u\, z(u) + Y(u)\,] \cos\left(u \ln \frac{A}{r} \right) \right] \frac{du}{1+u^2}$$

$$\frac{\pi r}{2AT_0}\tau_{r\theta} = \int_0^\infty [\, \theta(u) + uX(u)\,] \left[\cos\left(u \ln \frac{A}{r} \right) + u \sin\left(u \ln \frac{A}{r} \right) \right] \frac{du}{1+u^2}$$

where,

$$\theta(u) = \cos(\alpha + \theta)\cosh(\alpha - \theta)u + \cos(\alpha - \theta)\cosh(\alpha + \theta)u$$
$$Y(u) = \sin(\alpha - \theta)\sinh(\alpha + \theta)u + \sin(\alpha + \theta)\sinh(\alpha - \theta)u$$
$$X(u) = \cos(\alpha - \theta)\sinh(\alpha + \theta)u - \cos(\alpha + \theta)\sin h(\alpha - \theta)u$$
$$z(u) = \sin(\alpha + \theta)\cosh(\alpha - \theta)u - \sin(\alpha - \theta)\cos h(\alpha + \theta)u$$

These equations for the stress distribution were again evaluated for wedge angles of $2\alpha = 60^\circ$ and $2\alpha = 90^\circ$. Figure (10) shows the isochromatic lines produced by this system of loading. High order of maximum shear

stress is seen to occur around the points on the wedge face at $\frac{r}{A} = 1$. The neutral axis originates at the apex and coincides with the axis of symmetry. The features of this isochromatic pattern are similar to those observed in photoelastic experiments with point loading at the apex[11].

III – Superposition of the Normal Pressure and Shear-stress Solutions to Simulate the Stress Boundary Conditions on a Scoring Tool:

The normal pressure and shear stress solutions are superimposed to simulate the stress boundary conditions on a Wedge indenter. However, from plasticity analysis (Ref 6) it is evident that with increasing ratio of shear stress to normal pressure a limit occurs when the frictional stress T_c reaches the shear yield stress 'K' of the indented material. For a wedge of 10° included angle, this limit is reached at a ratio of 0.359, whereas for a wedge of 40° the limit is reached at a ratio of 0.27. Wide-angled wedges are limited by the formation of a dead metal nose (Ref. 6). Therefore, to simulate the indentation process a ratio of shear stress to normal pressure equal to 0.2 would appear to be fairly representative of wedge indentation process. This ratio is high enough to show the influence of frictional stresses and low enough not to exceed the fore-mentioned limitations. In this section, a solution for combined shear stress and normal pressure in the ratio 0.2 is obtained by superposition of previous solutions for P_0 and

$T_0 = \frac{1}{5} P_0$ acting over a distance 'A' from the wedge apex .

Figure (11) shows the resulting isochromatic lines obtained for the case of a 90° wedge under the combined effect of normal pressure and shear stress. An interesting feature of this pattern is the presence of maximum shear stresses along the wedge face at r = A. The effect of frictional stress is also to shift the position of neutral axis towards the apex.

Figures (12) and (13) show the distribution of rectangular stress components in a 60° and 90° wedges respectively. The effect of frictional stress is to induce more compressive stress to both σ_x and σ_y without much effect on the shape of the curves.

4– CONCLUSIONS

Previous investigators showed that during the indentation process of semi – infinite plastic rigid material by sharp wedge indenter, the faces of the wedge will be subjected to uniform normal and tangential stresses. In this paper the stress distribution in a wedge when subjected to such boundary conditions has been examined. It is possible from the present theoretical solution to predict the influence of frictional stresses on the distibution of stresses in the wedge. Comparison of theoretical results with photoelastic results will be presented in later work.

REFERENCEC

1 – B. Dodd
Ph. D Thesis, Birmingham University 1973

2 – Metal Box Companv. U. K. Patent No 1249687–Inventors J. T Franck and Peter Rhodes.

3 – C T Tranter
The Use of Mellin Transform in finding the Stress Distribution in an Infinite Wedge.
Quart. Jour. Mech. Applied Math
(Oxford), 1, 125, 1948

4 – M I Ghobrial
A Theoretical Investigation on the Distribution of Stresses in an Infinite Wedge Subjected to Uniform Tangential Boundary Loads . . . .
Sc. Journal, U. Technology 1980 ,4

5 – R Hill, E H Lee and S J Tupper
The theory of Wedge Indentation of Ductile Material
Proc. Roy. Soc. A. 188, 1947

6 – J Grunzweig , I M Longman and N J Petch
Calculations and Measurements on Wedge Indentation.
J. Mech Phys. Solids 2, 81, 1953

7 – W Johnson, F Mahtab and J B Haddow
The Indentation of a Semi–infinite Block by a Wedge of Comparable Hardness.
Int. J. Mech. Sci 6, 329, 1964

8 – T O Mulhearn
The Deformation of Metals by a Vickers-type Pyramidal Indenter.
J. Mech. Phys. Solids 7, 85, 1958

9 – D March
Plastic Flow in Glass
Proc . Roy. Soc. A, 279 , 470 , 1964

10– W Hirst and M Howse
The Indentation of Material by Wedges .
Proc . Roy . Soc. A, 311 , 429 , 1969

11– M M Frocht
Photoelasticity , Vol 1l
john Wiley and Sons .

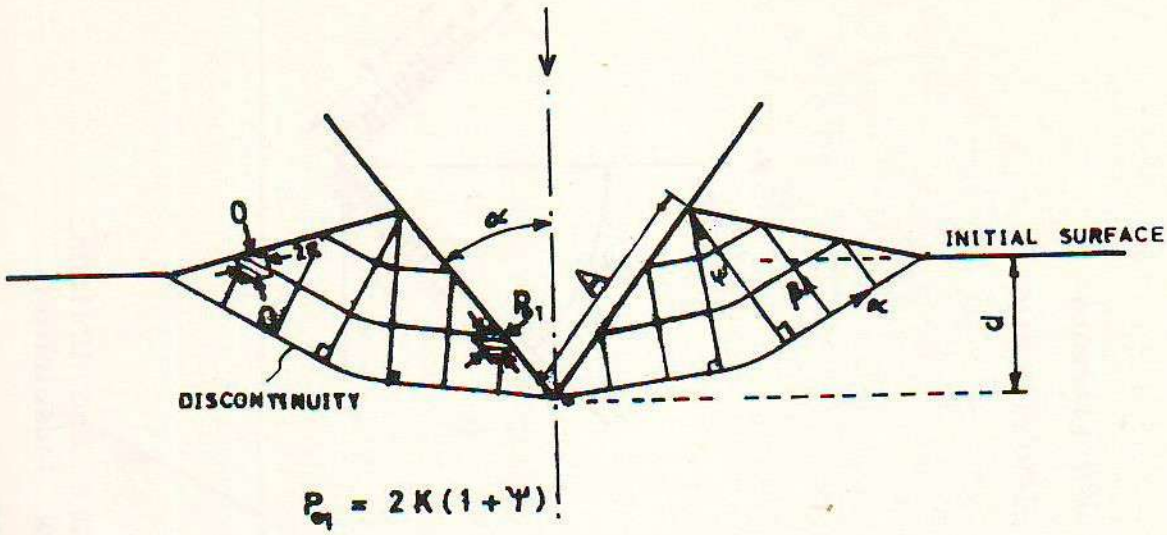

Fig.1 FRICTIONLESS WEDGE INDENTATION

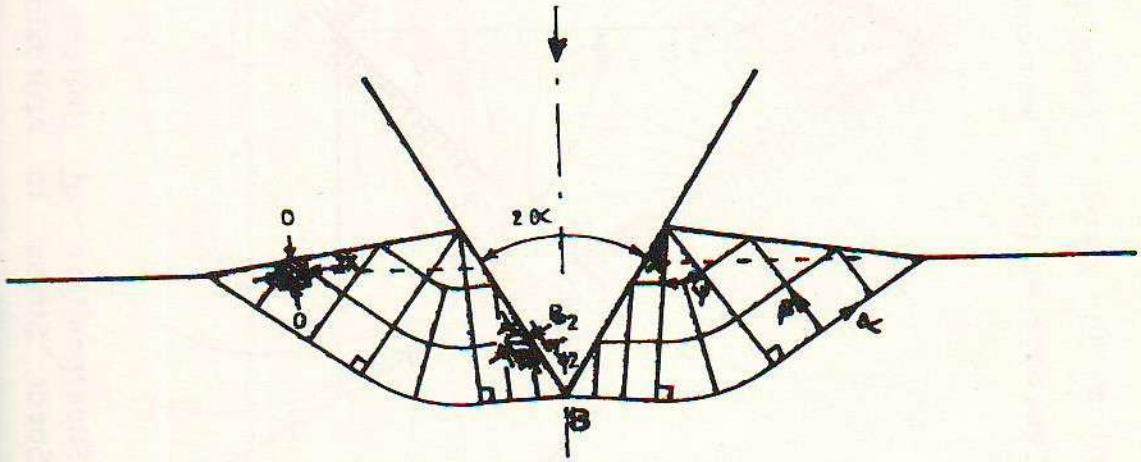

Fig. 2 ROUGH (COULOMB FRICTION) WEDGE INDENTATION

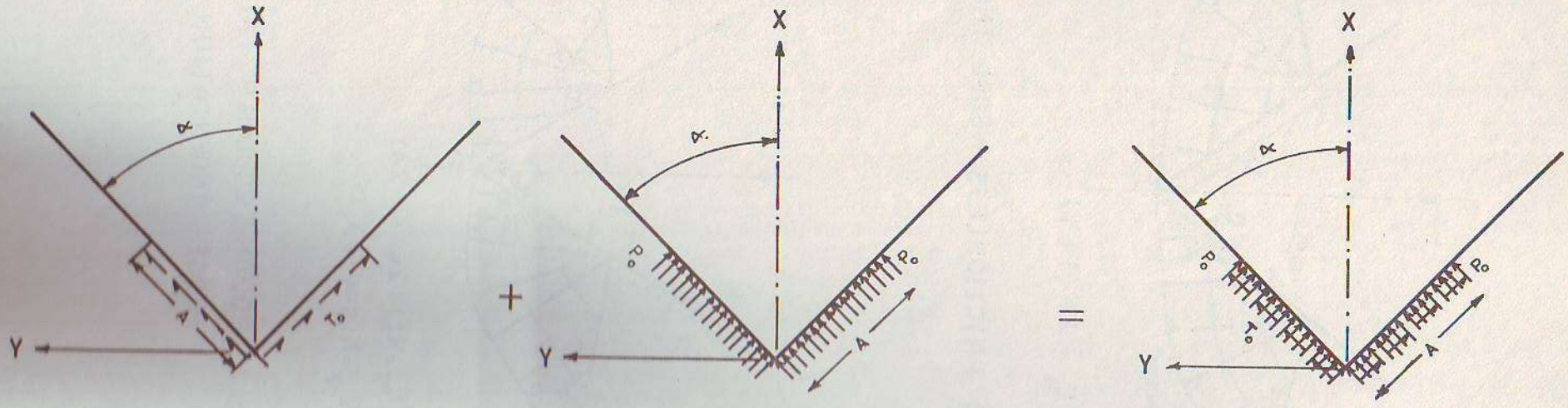

Fig. 3 Superposition of Uniform Normal Pressure And Uniform Shear Stress to Approximate Rough Wedge Indentation.

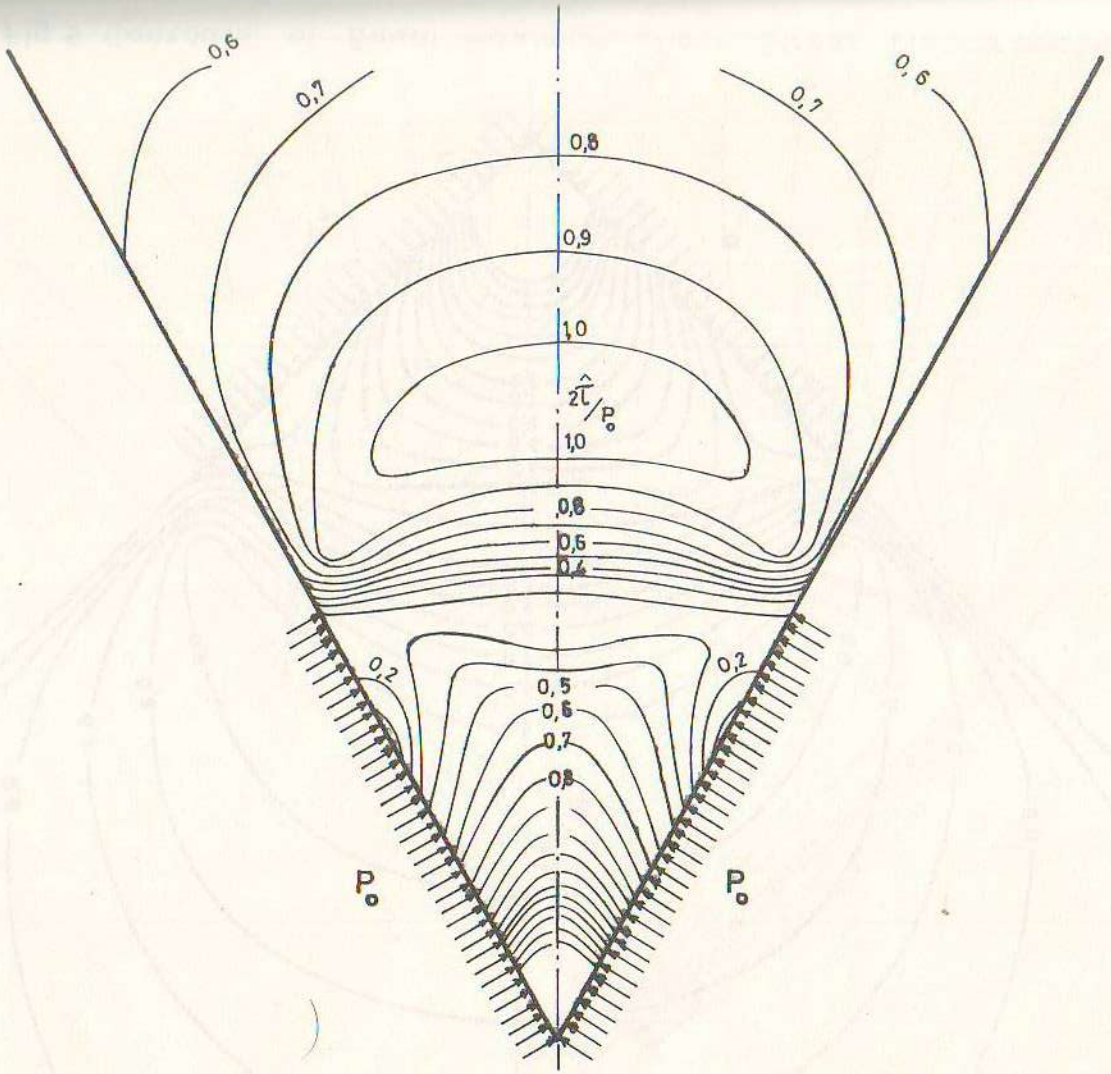

Fig. 4 Contours of Equal Maximum Shear Stress (Isochromatics) in a 60° Wedge, Loaded by Uniform Normal Pressure.

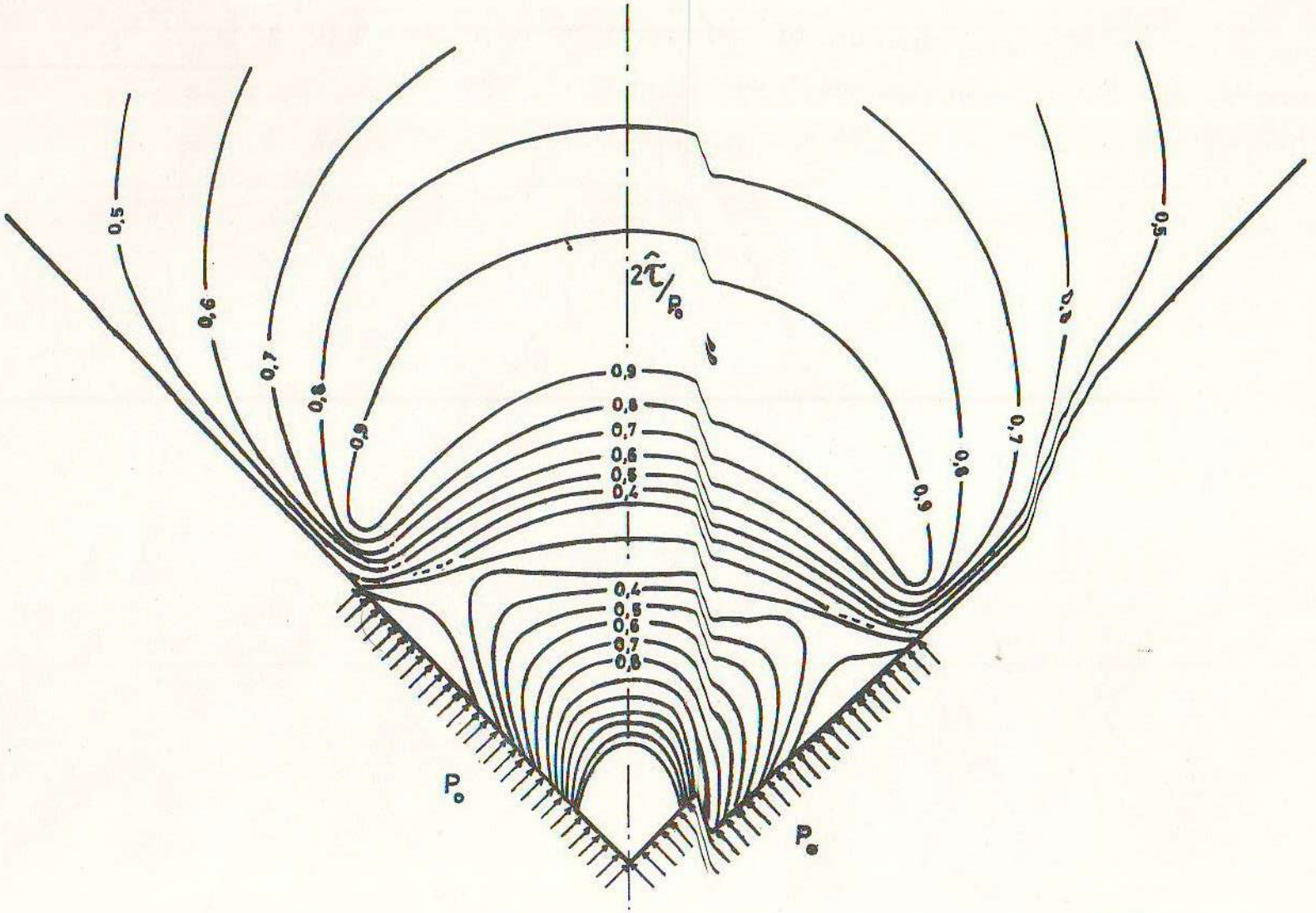

Fig. 5 Contours of Equal Maximum

in a 90° Wedge, Loaded by Shéar Stress (Isochromatics)

Uniform Normal Pressure

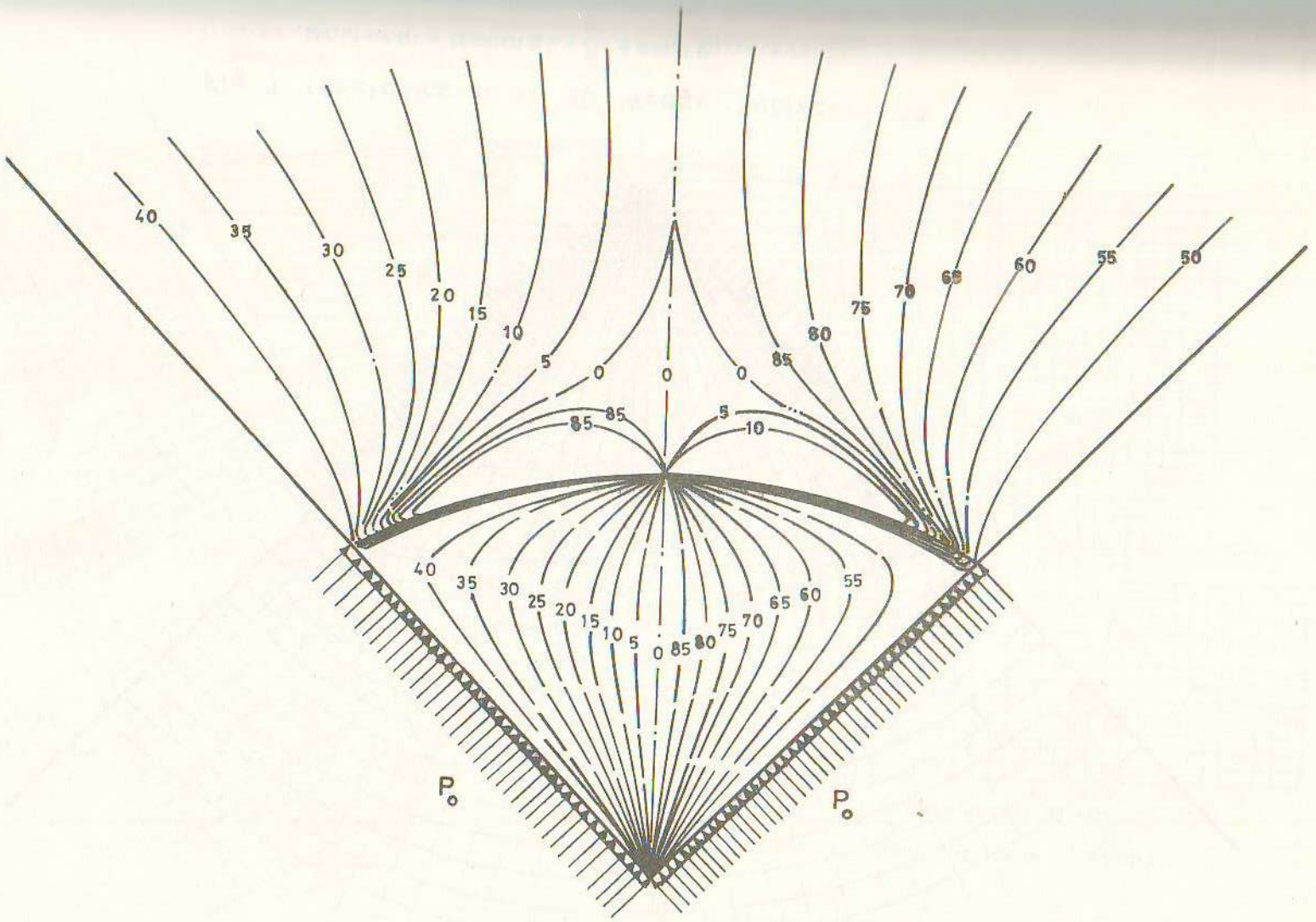

Fig. 6 Isoclinics in a 90° Wedge
Subjected to Uniform Normal Pressure

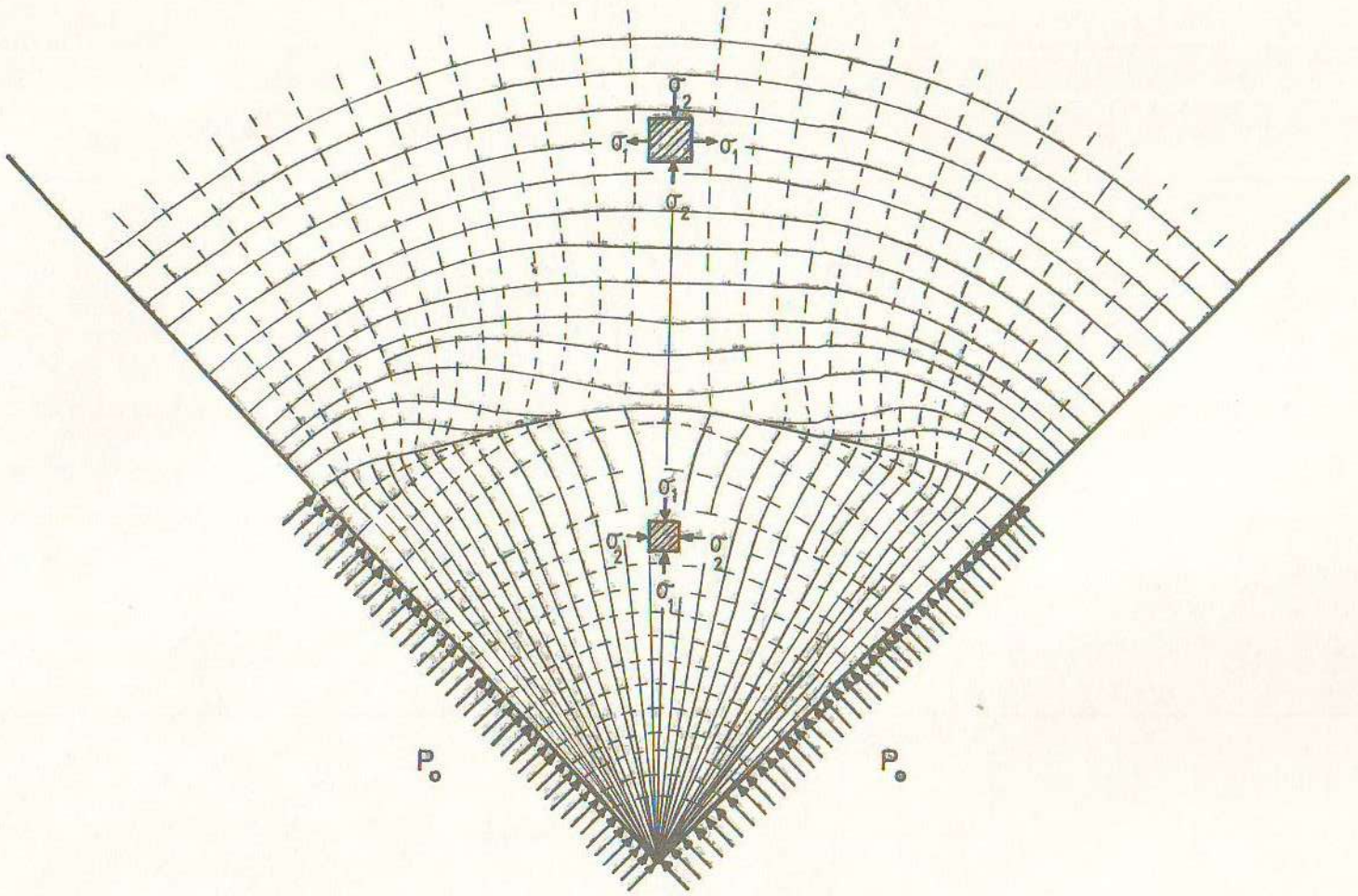

Fig. 7 Isostatics in a 90° Wedge Subjected to Uniform Normal Pressure.

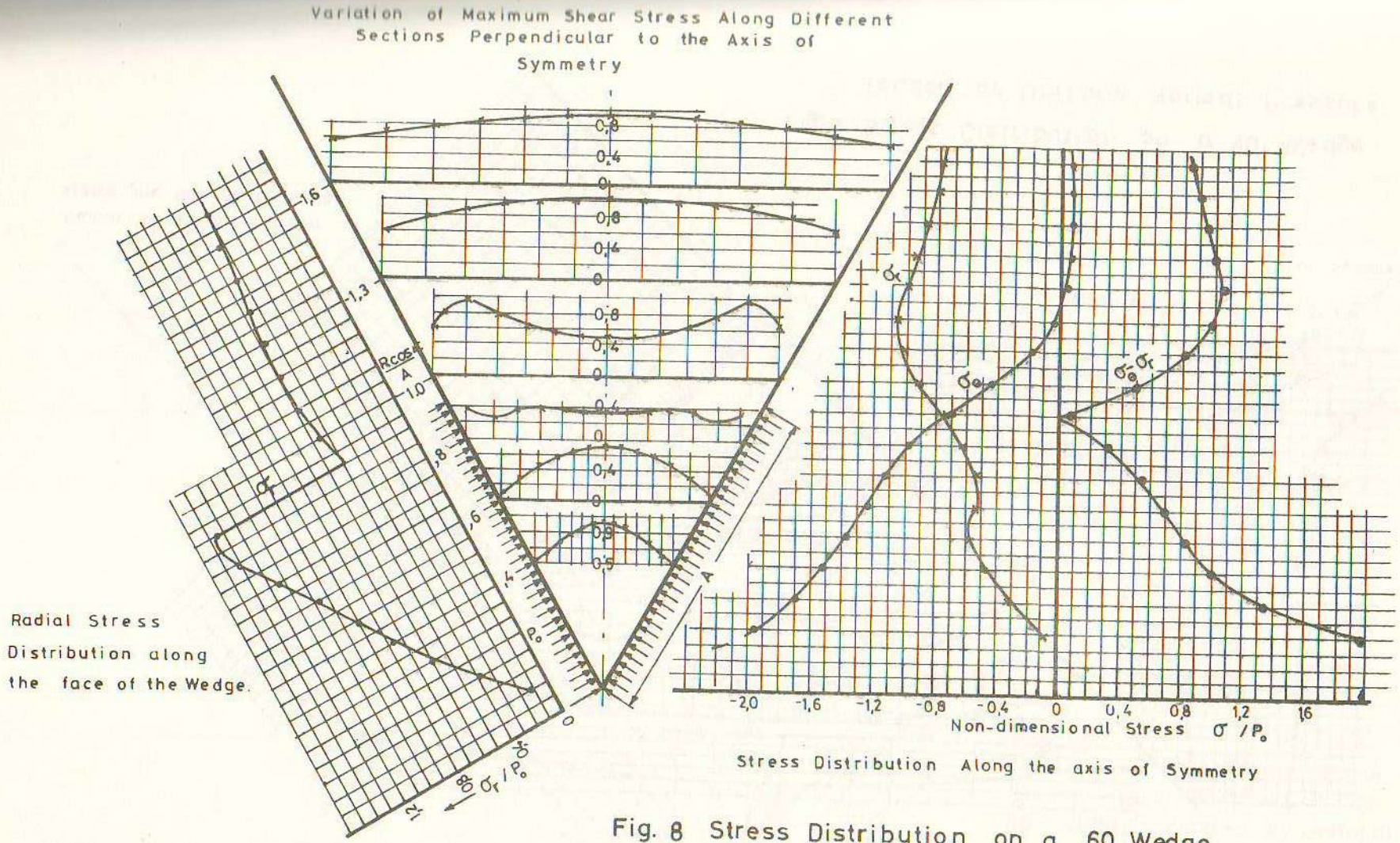

Fig. 8 Stress Distribution on a 60 Wedge Loaded by Uniform Normal Pressure.

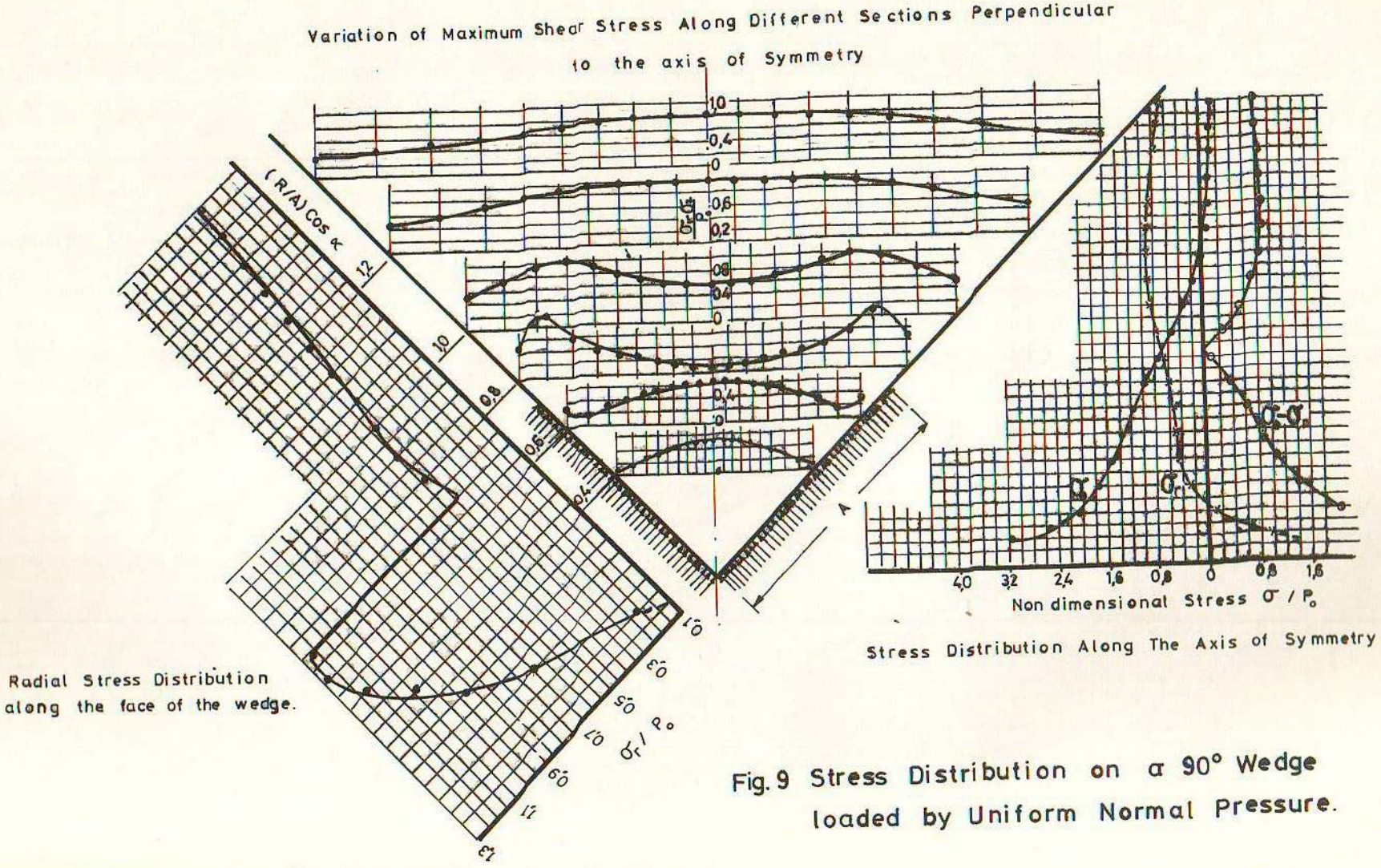

Fig. 9 Stress Distribution on a 90° Wedge loaded by Uniform Normal Pressure.

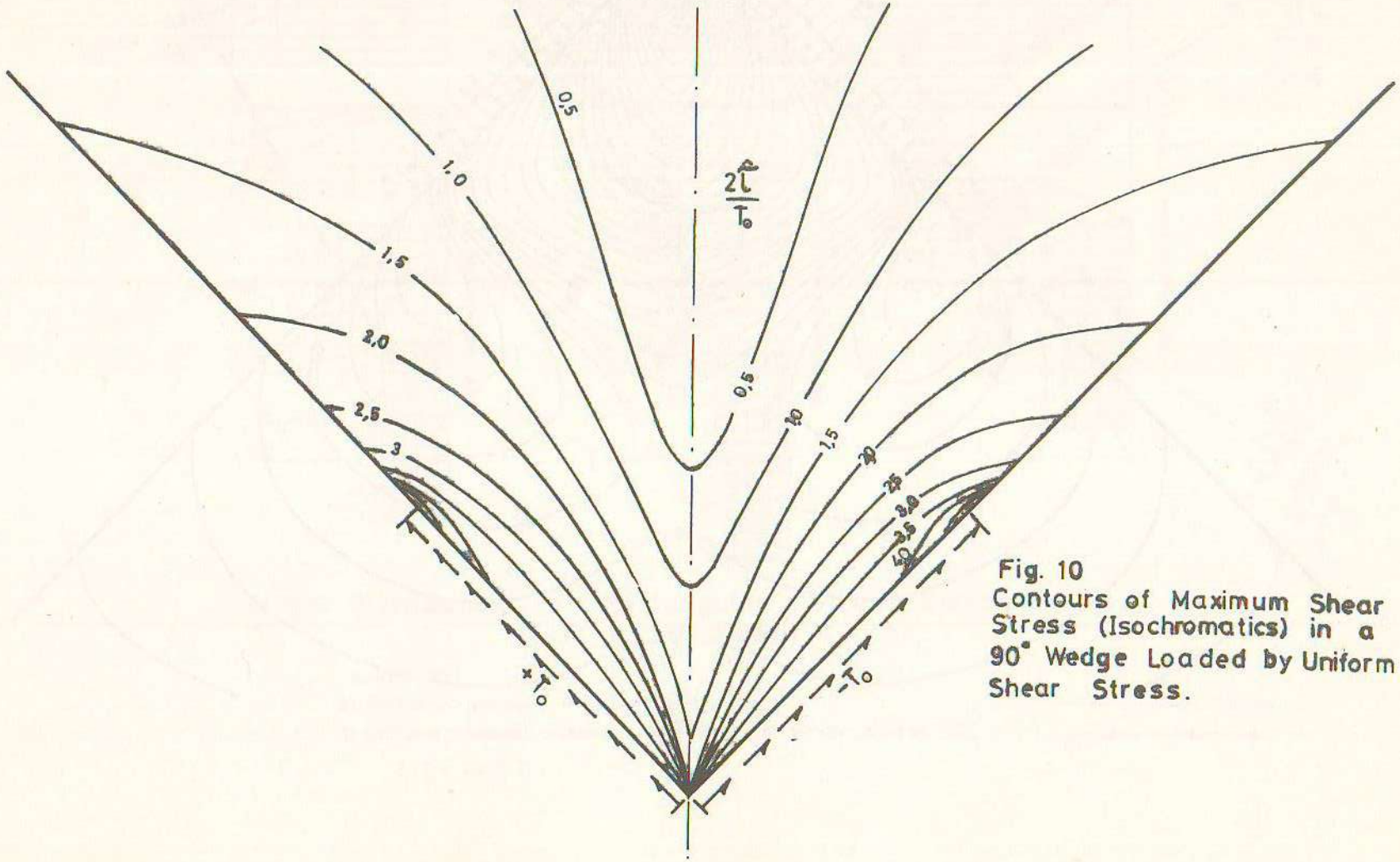

Fig. 10
Contours of Maximum Shear Stress (Isochromatics) in a 90° Wedge Loaded by Uniform Shear Stress.

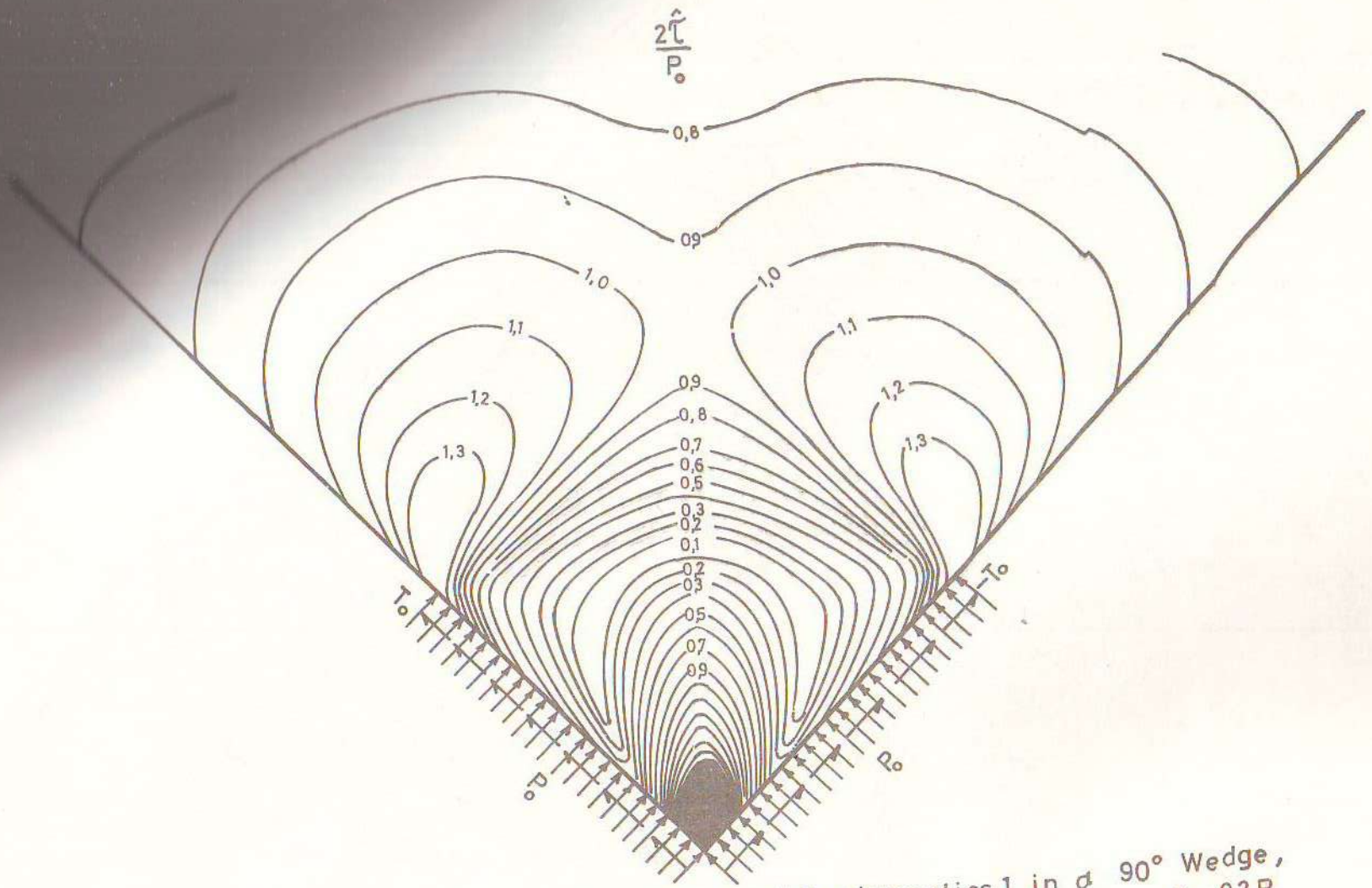

Fig. 11 Contours of Equal Maximum Shear Stress [Isochromatics] in a 90° Wedge, Loaded by Uniform Normal Pressure P_0 and Uniform Shear Stress $\tau_0 = 0{,}2\,P_0$

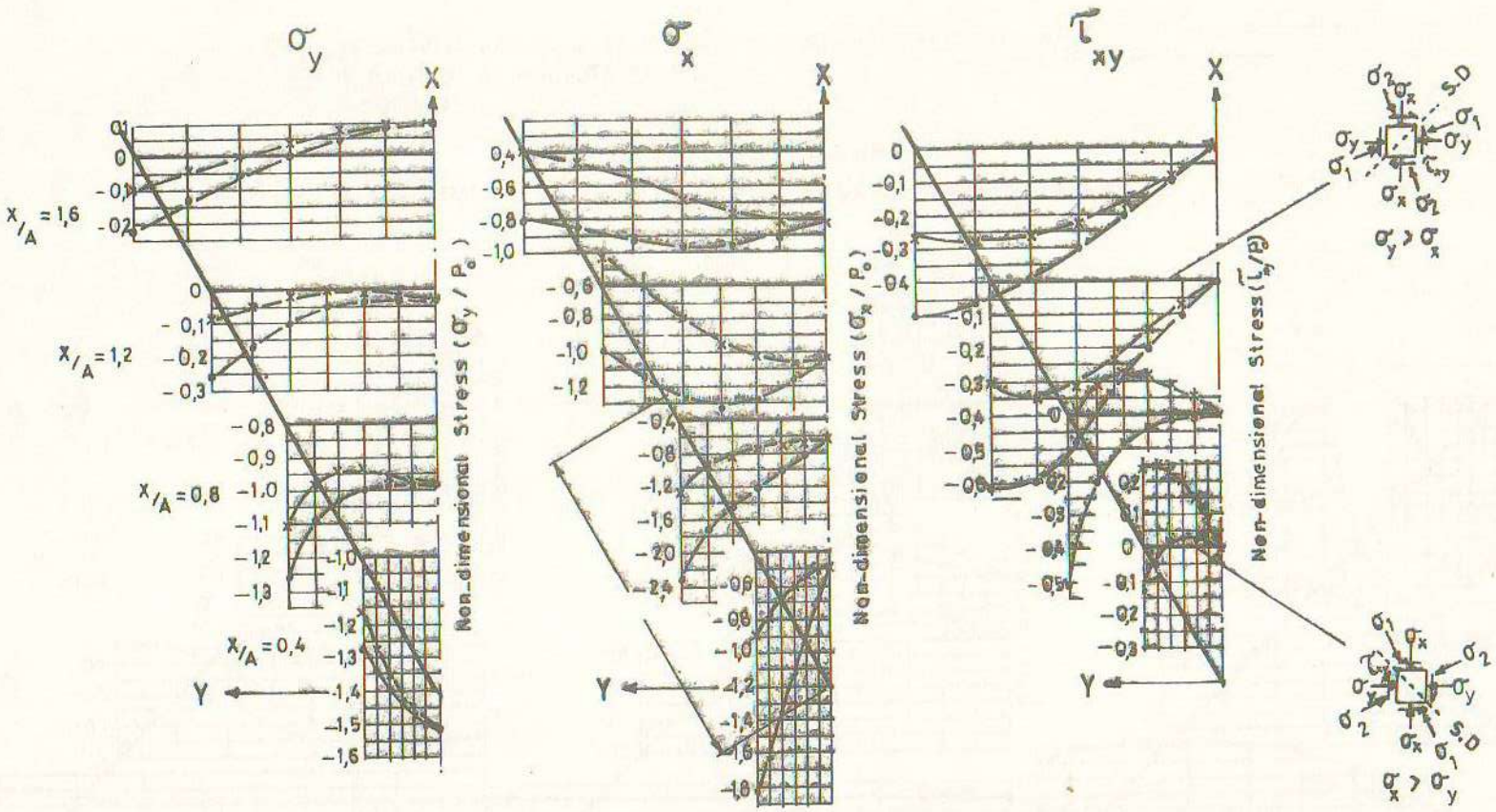

Fig 12 Distribution of Rectangular Stress Components in a 60° Wedge

LOADED BY:

a) Uniform Normal Pressure 'P_o'

b) Uniform Normal Pressure and Uniform Shear Stress 'T_o'

[$T_o = 0{,}2\ P_o$]

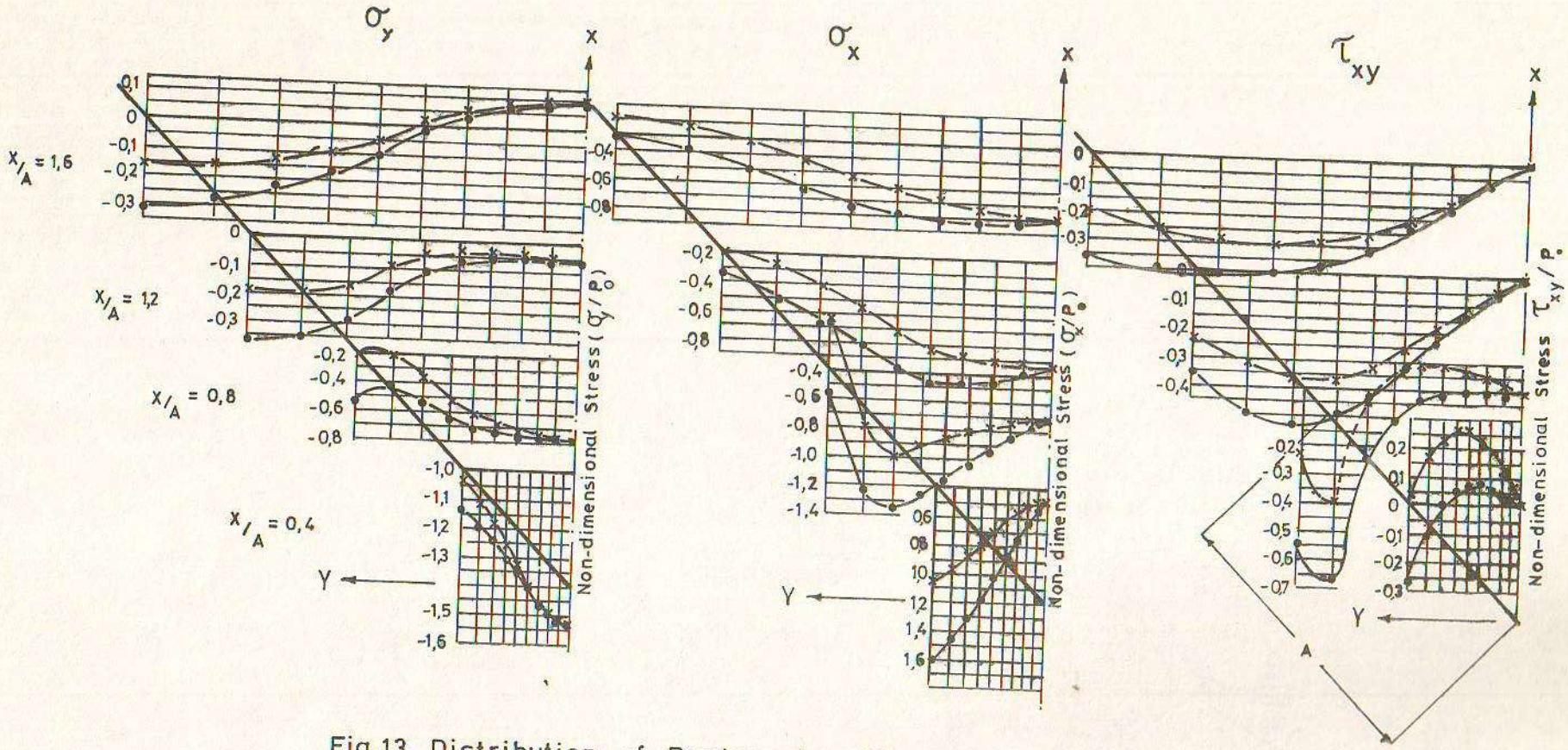

Fig.13 Distribution of Rectangular Stress Components in a 90° Wedge.

LOADED BY :
a) Uniform Normal Pressure 'P'
b) Uniform Normal Pressure 'P_o' and Uniform Shear Stress 'T_o'